NeuroImage 162 (2017) 23–31

Contents lists available at ScienceDirect

NeuroImage

journal homepage: www.elsevier.com/locate/neuroimage

Neurophysiological evidence for enhanced tactile acuity in early blindness in some but not all haptic tasks

Ane Gurtubay-Antolin [a,b,*], Antoni Rodríguez-Fornells [a,b,c]

[a] Cognition and Brain Plasticity Group, Bellvitge Biomedical Research Institute- IDIBELL, 08097, L'Hospitalet de Llobregat, Barcelona, Spain
[b] Dept. of Cognition, Development and Education Psychology, Campus Bellvitge, University of Barcelona, L'Hospitalet de Llobregat, Barcelona 08097, Spain
[c] Catalan Institution for Research and Advanced Studies (ICREA), 08010, Barcelona, Spain

ARTICLE INFO

Keywords:
Blindness
Haptic object recognition (HOR)
Touch
Shape
Texture

ABSTRACT

Previous research assessing the presence of enhanced tactile skills in early-blind (EB) population obtained conflicting results. Most of the studies relied on behavioral measures with which different mechanisms leading to the same outcome go unnoticed. Moreover, the scarce electrophysiological research that has been conducted focused exclusively on the processing of microgeometric properties. To clarify the extent of superior tactile abilities in EBs using high-density multichannel electrophysiological recordings, the present study compared the electrophysiological correlates of EBs and sighted controls (CON) in two tactile discrimination tasks that targeted microgeometric (texture) and macrogeometric (shape) properties. After a restricted exploration (haptic glance), participants judged whether a touched stimulus corresponded to an expected stimulus whose name had been previously presented aurally. In the texture discrimination task, differences between groups emerged at ~75 ms (early perceptual processing stages) whereas we found no between-group differences during shape discrimination. Furthermore, for the first time, we were able to determine the latency at which EBs started to discriminate micro- (EB: 170 ms; CON: 230 ms) and macrogeometric (EB: 250 ms; CON: 270 ms) properties. Altogether, the results suggest different electrophysiological signatures during texture (but not shape) discrimination in EBs, possibly due to cortical reorganization in occipital areas and their increased connectivity with S1.

1. Introduction

Neural and behavioral consequences of blindness are still under debate. On one hand, visual deprivation is related to the atrophy of elements of the visual system (Pan et al., 2007; Noppeney et al., 2005) which may lead to perceptual maladjustments in the remaining modalities, in particular those with spatial components (e.g., audition and touch). Since localization tasks in these senses benefit from visual calibration, it has been observed that blind Braille readers tend to mislocate tactile stimuli (Sterr et al., 2003) and perform worse in sound localization tasks (Lewald, 2002). Moreover, unsighted children underperform in haptic orientation discrimination (Gori et al., 2010) and auditory spatial tasks (Gori et al., 2013; Vercillo et al., 2016; Cappagli et al., 2017). On the other hand, it is assumed that a sensory deficit will lead to enhanced abilities when using the spared senses as a consequence of cortical reorganization in regions associated with the spared modalities as well as in areas initially responsible for the absent sense. In this line, superior performance of EBs compared to sighted individuals has been described in grating orientation tasks (Van Boven, Hamilton, Kauffman, Keenan and Pascual-Leone, 2000; Goldreich and Kanics, 2003), vibrotactile perception (Wan et al., 2010), 2D-angle differentiation tasks with a predefined exploration (Alary et al., 2008) and discrimination of surfaces with raised dots (Alary et al., 2009). However, other studies assessing the presence of enhanced tactile skills in EB population obtained alternative results. EBs were not found to outperform in orientation discrimination of gratings, vibrotactile perception, discrimination of braille-like dot patterns (Alary et al., 2009; Grant et al., 2000) or smoothness judgments with active or passive exploration (Heller, 1989).

Several authors point to individual differences in the use of exploratory strategies and to task-specific effects as an explanation for the discrepant results obtained by the previous studies. Even considering that the natural strategies for acquiring somatosensory information about texture and shape are *lateral motion* and *contour following* (Lederman and Klatzky, 1987), a brief haptic exposure without active exploration

* Corresponding author. Cognition and Brain Plasticity Unit, IDIBELL University of Barcelona, Basic Psychology Dept., Bellvitge Campus, University of Barcelona, L'Hospitalet de Llobregat, Barcelona, 08097, Spain.
E-mail address: anegurtubay@gmail.com (A. Gurtubay-Antolin).

http://dx.doi.org/10.1016/j.neuroimage.2017.08.054
Received 15 July 2017; Received in revised form 11 August 2017; Accepted 20 August 2017
Available online 24 August 2017

(termed 'haptic glance'), (Klatzky and Lederman, 1995) is enough to identify previously presented stimuli eliminating individual differences in the exploration. Likewise, a superior performance of EBs in certain tactile tasks is not mandatorily associated with possessing enhanced skills in all the tasks pertaining to the haptic modality. Taking into account that tactile object recognition seems to depend on parallel information processing of micro- (e.g. texture) and macrogeometric attributes (such as shape) (Bohlhalter et al., 2002), it is plausible that EBs show different abilities in the processing of micro- and macrogeometric properties. Differences between blind and sighted population in the preferred sensory modality to encode each type of property support this idea, since vision is the dominant sense to encode shape-relevant information in sighted population while both sighted and EBs use haptics to encode texture-related information (Lederman and Klatzky, 1987; Lederman et al., 1996).

Importantly, former studies investigating the presence of superior somatosensory abilities in EBs relied almost exclusively on behavioral measures and up to present, very few researches have analyzed the neurophysiological correlates of tactile processing in EBs. Brain electrical activity (assessed by event-related brain potentials, ERPs) may contribute in the clarification of the results for various reasons. First, plasticity mechanisms may be present at multiple levels (e.g. molecular, neural or behavioral). Thus, superior tactile abilities (such as a higher speed of somatosensory processing in EBs compared to sighted) may be identified at the neurophysiological level despite not leading to different performance between groups. Second, neurophysiological data can provide temporal and topographical information of events assessing differences in the mechanisms underlying haptic discrimination in each group as well as identifying the processing stage at which EBs process tactile information distinct to sighted.

Seminal work investigating haptic processing in blind population using electrophysiological measures revealed that blind individuals presented shorter latencies in the somatosensory N1 event-related potential (ERP) component during a tactile oddball task with Braille-like dotted patterns (Roder et al., 1996). This result suggests a more efficient processing of information in the blind group in this modality. However, this research pooled together early- and late-blind participants, whose neural development has been seen to vary moderately between them since the extent of cortical reorganization depends on the timing of the onset of blindness (Voss et al., 2010; Merabet and Pascual-Leone, 2010). In addition, results obtained in a tactile spatial attention task determined that EBs differed between attended and non-attended vibrotactile stimuli 6 ms earlier than sighted population as indexed by the peak amplitude of the P100 component (Forster et al., 2007). To note, the stimuli used in the former electrophysiological studies focused on microgeometric properties and no research has yet focused on the tactile processing of macrogeometric properties in EBs, in order to compare the processing of both types of attributes.

The purpose of the present study was to investigate for the first time whether a group of EBs and sighted participants showed similar electrophysiological correlates in two haptic discrimination tasks targeting microgeometric (texture) and macrogeometric (shape) properties. Importantly, the use of high-density multichannel EEG recordings (64 locations) permitted a more precise delineation of cortical activity compared to previous work. Furthermore, restricted exploratory procedures have enable to control for individual differences in the exploratory procedures. In line with previously reported results, we expected the EB group to show a reduction in the time required for texture discrimination, whereas we hypothesized that such temporal advantage could be reduced in the shape discrimination task (possibly due to the use of supplementary visual mechanisms in sighted controls).

2. Materials and methods

2.1. Participants

14 early blind (EB) (7 women, mean ± SD, age = 35.7 ± 10.9 years) and 15 sighted controls (CON) (9 women, mean age = 29.3 ± 9.0 years) took part in the experiment. The two groups were matched by age ($p = 0.1$) and years of education ($p = 0.8$). With the exception of one blind subject with well managed epilepsy, no subjects had neurological disorders. The inclusion criteria for the EB group included right handedness, less than 10% of visual residual abilities (as determined by ONCE standards for visual acuity and visual field), blindness onset before 5 years of age (the age at which synaptic density in the visual cortex reaches adult levels) (Johnson, 1997) and the ability to avoid blinks and to control eye movements for 3 s. The latter requirement was the most exclusive criterion and 8 EB subjects could not participate in the study due to it. The EB group was heterogeneous with respect to the degree of Braille reading and light perception level. Blindness of cerebral origin was an exclusion criterion (see Table 1 for further demographic information). Three congenitally blind participants were excluded from the ERP analysis and two of them were also excluded from the behavioral analysis. EB4 was only removed from the ERP analysis due to excessive muscular artifacts. She performed the tasks correctly so she was included in the behavioral analysis. EB10 was rejected from both the ERP and the behavioral analyses due to residual abilities to read with a very high contrast and magnifiers, despite reporting 3% of residual visual abilities. EB14 was also removed from both the ERP and the behavioral analyses because he did not perform the shape discrimination task for time reasons and consequently, we could not test differences between tasks. The experiment was undertaken with the understanding and written consent of each participant and was approved by the local ethics committee in accordance with the declaration of Helsinki.

Table 1
Demographic characteristics of early blind participants and control samples. The 'LP' column indicates whether the subjects have light perception. The 'onset' and 'duration' columns refer to the age of blindness onset and the duration of blindness until present (years). 'Education' represents the years of education. 'Braille duration' refers to the years spent reading Braille. 'Hrs/week Braille' details how many hours a week the subjects dedicate to Braille reading (at present). EB = Early blind, Con = sighted controls. M = Male, F = Female.

	Age & Gender	Cause of blindness	LP	Onset	Duration	Education	Braille duration	Hrs/week Braille
EB 1	24 M	Congenital glaucoma & retinal detachment	No	0	24	14	19	0
EB 2	30 F	Microphthalmia & Congenital cataracts	Yes	0	30	15	25	1
EB 3	28 F	Premature retinopathy	Yes	0	28	22	24	1
EB 4	30 F	Congenital glaucoma	Yes	0	30	12	26	0
EB 5	31 F	Leber's congenital amaurosis	Yes	0	31	19	25	3
EB 6	46 F	Atrophy of the optic nerve	No	1.5	44.5	23	41	6
EB 7	29 M	Bilateral retinoblastoma	No	4	25	24	24	10
EB 8	53 M	Atrophy of the optic nerve	No	0	53	7	37	1
EB 9	35 F	Bilateral retinoblastoma	No	4	31	20	30	1
EB 10	35 F	Bilateral retinoblastoma	Yes	1	34	19	–	–
EB 11	23 M	Premature retinopathy	No	0	23	20	19	0
EB 12	52 F	Bilateral retinoblastoma	No	0	50	36	47	14
EB 13	43 M	Premature retinopathy	Yes	0	43	19	38	40
EB 14	19 M	Bilateral retinoblastoma	No	0	19	16	15	1
Con	29 (±9) 9F	–	–	–	–	20 (±4)	–	–

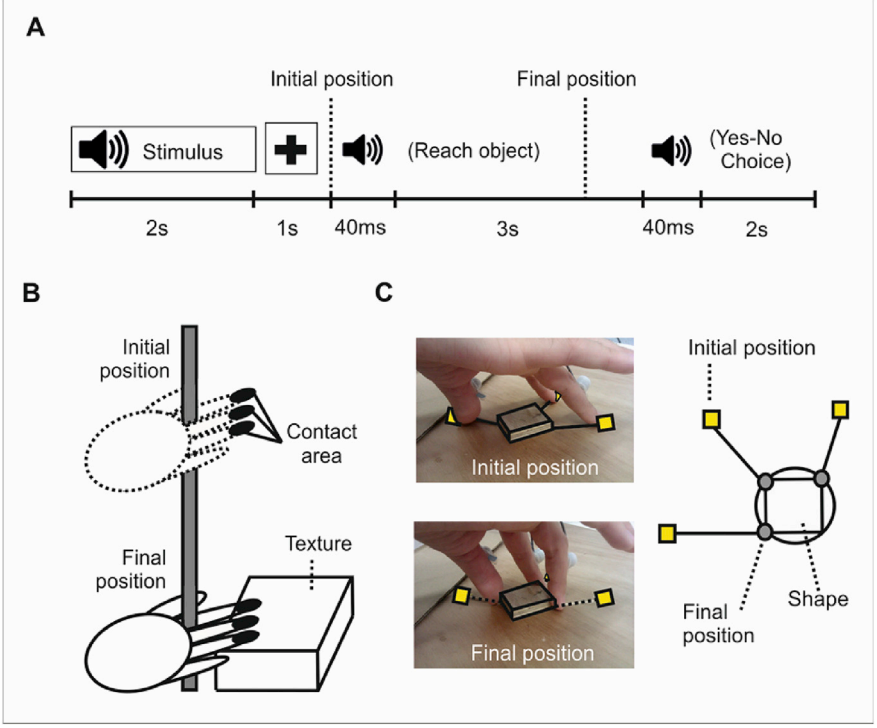

Fig. 1. A) Trial procedure with the duration of each step. B) Illustration of the exploratory procedure used in the texture-task: participants slid their hand through the vertical stick until touching the object with three fingertips –as an entity- and following the contact with the object they were not allowed to perform any movement. C) Photographs and illustration of the exploratory procedure used in the shape-task: the three fingers moved independently (see also Gurtubay-Antolin et al., 2015).

2.2. Haptic stimuli and procedure

Participants sat on a comfortable chair with the right arm extended on a table. In the texture-task, a wooden rectangle (size: 5 cm × 5 cm) was covered with ten textures (cotton, cork, sackcloth, sandpaper, sponge, scourer, corduroy, suede, paper and velvet). The texture-stimuli were selected according to previous research where the most dominant attribute to identify these objects was their texture (Lederman and Klatzky, 1990, 1993) and a texture-notebook used for cognitive-intervention purposes in Alzheimer patients (Peña-Casanova, 1999). Metallic materials were ruled out to exclude temperature as an informative factor. In the shape-task, ten previously used 2D wooden geometrical objects were manufactured: racket, circle, square, triangle, arrow, flower, crown, heart, star and lightning (see Gurtubay-Antolin et al., 2015). To note, the stimuli used in the shape and in the texture discrimination task were had similar sizes. This set of objects was chosen to be identifiable with only 3 contact points and at a single grasp. All the stimuli were easily identifiable based on the discriminability index (d'), which was above 1.79 in all cases. The discriminability index is defined as the standardized score of a hit minus the standardized value of a false alarm (hit: correct answer in a congruent trial – e.g. participant reports touching velvet when the expected texture is velvet; false alarm: incorrect answer in an incongruent trial –e.g. participant reports touching velvet when the expected texture is cotton). Sighted participants were not allowed to see the objects during the entire experimental study. We obstructed vision by placing an opaque screen between the subject and the object.

Prior to the experiment, participants underwent a learning-training phase to become familiar with the stimuli and learn to identify them. In this phase, free haptic exploration was allowed. Both experimental tasks had the same procedure (see Fig. 1a), and in order to minimize differences in the exploratory method, all participants conducted the same constrained exploration (haptic glance) which consisted in contact with the object with 3 fingertips for ~3 s. The only difference between the tasks was the haptic exploration used in order to identify the object. In the texture-experiment, participants touched the textures with the fingertips of the index, middle and annular fingers. They contacted the object following a vertical movement guided by a stick (see Fig. 1b). All three fingers were tied together in order to avoid any lateral motion along the surface to extract further information. In the shape discrimination task, the haptic exploration consisted in touching the shapes at three specific locations (*contact points*), after sliding three fingers (thumb, index and middle) through three rails that were attached to the table (see Fig. 1c). Contact points were the same for each object, preventing the use of their location to discriminate objects. Thus, the three fingers always had the same initial and final positions (more detailed information is presented in Gurtubay-Antolin et al., 2015).

At the beginning of each trial, subjects placed the fingers in the initial position. The name of one of the stimuli was delivered through headphones followed by a fixation cross (for sighted participants) for 1 s. Since the majority of the blind participants had light perception, a fixation light was used in order to avoid eye movements. An auditory cue was then presented for 40 ms, indicating that the three-finger movement towards the figure could begin. In the texture-task, participants slid their fingers through the vertical stick, and in the shape-task the fingers were moved along the three rails attached to the table, to reach the stimulus. In half of the trials the word delivered by the headphones corresponded to the object touched (congruent), and in the other 50% of trials the object did not match the name (incongruent). For each of the 10 objects, 9 repetitions of their congruent trial and 9 incongruent trials were presented. The incongruent trials were a combination of each stimulus (e.g 'Stimulus 1') with the remaining stimuli (e.g. 'Stimulus 1'-'Stimulus 2', 'Stimulus 1'-'Stimulus 3', …, 'Stimulus 1'-'Stimulus 10', with the former stimulus the one heard through the headphones and the latter, the touched object). All the trials were randomly presented. Three seconds after the first auditory cue a second auditory cue indicated that a response had to be emitted, requesting the participants to press 'Yes' or 'No', considering whether the object that they were touching corresponded to the name of the previously heard object (see Fig. 1a). Participants were requested to delay their motor response for 3s in order to avoid contamination of the EEG signal from motor related ERP-

components. The Yes-No choice was made by pressing one of two keyboard buttons with the left hand. The response button was counterbalanced across participants.

The experimental session consisted of 180 trials performed in 4 different blocks, interleaved by resting periods. Each block consisted of three series of 15 trials. The total duration of each experiment was approximately 80 min. Finger movements were recorded using an infrared motion capture system (CMS-30P, Zebris, Isny, Germany) with a spatial resolution of 0.1 mm to measure the time at which subjects reached the object (contact time). A sampling frequency of 200 Hz was used in the texture-task and 66 Hz in the shape-task. The difference between the sampling frequencies of the movement recording in the two tasks is due to the number sensors that are necessary to record the movements of the fingers. Since the three fingers were tied together in the texture modality in order to prevent lateral movements along the surface, the three fingers moved like an entity and only one sensor was required. In contrast, each finger moved independently in the shape modality, and thus three sensors were attached to the three fingers of the subject's right hand. Data recording began 100 ms before the auditory cue and ended 3 s after. Contact-time with the object (CT) was defined as the time when the absolute velocity of the first finger reaching the object was lower than 5% of its peak velocity. The use of different exploratory procedures in each task renders it impossible to compare the time course of somatosensory processing between tasks. In the texture task, the three fingers exploring the object moved as an entity and no movement was performed after *contact-time,* isolating the somatosensory processing in the ERPs. In contrast, the three fingers moved independently in the shape discrimination task, and since *contact-time* was defined as the arrival of the first finger to the object, further movements (corresponding to the arrival of the second and the third fingers) were executed after *contact-time*. Hence, in the shape task, the ERPs reflected motor execution (of the last two fingers to reach the object) in addition to somatosensory processing. Importantly, we could have chosen to define contact-time as the last finger reaching the object (as we did indeed in our previous study, Gurtubay-Antolin et al., 2015). However, triggering ERP responses based on the last contacted finger did not reflect information related to early somatosensory processing occurring after the first two fingers contacted the object. Notice that the information provided by the first two fingers when contacting the object might be crucial in incongruent trials where the first two fingers could provide sufficient information to classify the trial as an incongruent trial.

2.3. Behavioral analysis

As we sought to have as many trials as possible in order to obtain reliable averages for the electrophysiological analysis, we required participants to be very accurate. Participants' data was only analyzed when a minimum threshold of correct responses was achieved during the training phase: 87% and 90%, for the texture and the shape task respectively. The number of correct responses was entered into a mixed model ANOVA with two within-subject factors [congruency (congruent vs. incongruent) and task (texture vs. shape)] and a between-subjects variable [group (controls vs. EB)]. Since differences between groups in the number of correct responses might not arise because the accuracy was forced to be extremely high, we decided to assess differences on the discriminability index (for which no threshold was required). We conducted a two-way repeated measures ANOVA on the discriminability index with 'group' and 'task' as factors. In case marginally significant interactions were found, within subject related samples *t*-test where conducted between tasks.

2.4. Multichannel EEG recordings and analysis

High-density EEG recordings were acquired from 64 scalp electrodes (Electro-Cap International) using Brain-Vision Recorder software (version 1.3; Brain Products, Munich, Germany). Data was analyzed with EEGLAB (Delorme and Makeig, 2004) and MATLAB (The Mathworks, Inc., Munich, Germany). In addition, we used FieldTrip (http://www.ru.nl/neuroimaging/fieldtrip) (Oostenveld et al., 2011) to run cluster-based permutation tests on the data. Electrode positions were based on the standard 10/20 positions (Jasper, 1958): Fpz/1/2, AF3/4, Fz/1/2/3/4/5/6/7/8, FCz/1/2/3/4/5/6, Cz,/1/2/3/4/5/6, T7/8, CPz/1/2/3/4/5/6, Tp7/8, Pz/1/2/3/4/5/6/7/8, POz/1/2/3/4/5/6, Oz/1/2. Trials with incorrect responses or with a response-time higher than 2s were removed from the analysis. Eye movements and blinks were monitored by electrodes placed on the external canthus and the infraorbital ridge of the right eye. All scalp electrodes were referenced offline to the average of the reference electrodes, placed at the right and left mastoid. Electrode impedances were kept below 5 kΩ. The EEG signal was sampled at 250 Hz and filtered with a bandpass of 0.03–45 Hz (half-amplitude cut-offs). Trials with base-to-peak electrooculogram (EOG) amplitude of more than 75 μV, amplifier saturation, or a baseline shift exceeding 200 μV/s were automatically rejected (Cunillera et al., 2008). These criteria removed electrocardiogram (ECG) contamination in most of the participants. After visually inspecting all the trials and in order to remove trials with remaining ocular artifacts, independent component analysis (ICA) (Delorme et al., 2007) was conducted in three subjects where the previous rejection was not enough to remove ECG contamination. Again, all extracted epochs were visually inspected. Contact-locked ERPs for artifact-free trials (in the (i) congruent, (ii) incongruent and (iii) all -congruent + incongruent-conditions) were averaged over epochs of 850 ms, from 50 ms pre-contact to 800 ms post-contact. To obtain reliable averages, we required each congruency condition to have a minimum of 50 trials per participant.

Due to fundamental differences in the exploratory method, we analyzed each task separately. From the entire set of scalp electrodes, we selected 45 electrodes that excluded frontopolar and anterior frontal electrodes as well as electrodes in the edges of the cap (F7/8, T7/8, Tp7/8, P7/8) since muscular artifacts (neck rigidity and facial tension) usually affect these sites. In each task, we submitted amplitude values where the difference between congruent and incongruent trials seemed maximum (texture: 200–400 ms interval; shape: 300–500 ms) to a mixed-model ANOVA with two within-subject factors [congruency (congruent vs. incongruent) and electrode (45 levels)] and a between-subjects variable (group). Based on previous results obtained in the same shape-experiment (where the 'electrode' x 'congruency' interaction was found to be highly significant) (Gurtubay-Antolin et al., 2015) we expected to find similar results suggesting differences in the topographical distribution of the incongruency effect. When the assumption of sphericity was not met the Greenhouse-Geisser correction was applied (Jennings and Wood, 1976) when the epsilon estimate of sphericity was lower than 0.75 (Girden, 1992). For full disclosure, the Huyhn-Feldt correction (Huynh and Feldt, 1976) is also reported in case the results differed between both types of correction. The p-values under these corrections are reported as p_{GG} and p_{HF} respectively. In case a significant interaction with the 'electrode' factor was found, the electrodes were assumed to be independent between them. Likewise, in case a significant interaction involving the factor 'group' was found, we proceeded to analyse each group separately.

Within each group and for each task separately, the onset and offset latencies of the incongruency effect (latency at which both congruency conditions start to differ) for each electrode were determined via a stepwise series of one-tailed serial t-tests (step size = 4 ms). The onset latencies were defined as the point at which more than 10 consecutive t-tests showed a significant difference from zero ($t = 2.063$) (Gurtubay-Antolin et al., 2015). In addition, we analyzed the topographical distribution of the voltage within the 100 ms time-window following the onset of the incongruence effect and we run cluster-based permutation tests on the data to control the family-wise error rate due to multiple testing (Maris and Oostenveld, 2007). First both conditions (congruent and incongruent) were compared for every sample (channel, time) with a dependent samples *t*-test. All samples with a t-value larger than 0.05 were

selected and then clustered on the basis of temporal and spatial adjacency. Taking the sum of the t-values within every cluster, cluster-level statistics were calculated and the maximum was taken as the test statistic to evaluate the effect of the experimental conditions in that time-window (100 ms interval after the onset of the incongruence effect). The Monte Carlo method with 1000 random draws was used to calculate the significance probability and identify significant clusters with a p-value under the critical alpha-level of 0.05.

To derive a topographical visualization of the voltage sources, we transformed the contact-locked averaged ERP waveforms into reference-free current source density (CSD) estimates (in $\mu V/cm^2$, head radius = 10 cm) (Perrin et al., 1989; Kayser and Tenke, 2006) and focused on the CSD estimates in a 100 ms time-window after the onset of the incongruency effect. The same procedure was used to address differences between groups in each task. The onset latency of the differences between groups was again defined as the point at which more than 10 consecutive t-tests showed a significant difference from zero and the topographical distribution of the voltage within the 100 ms time-window following the onset of the differences was analyzed. Again in case differences were found, we focused on the CSD estimates in a 100 ms time-window after the onset of differences between groups. In order to analyse the topographical distribution, cluster-based permutation tests were also applied to the CSD estimates.

3. Results

3.1. Behavioral results

The number of correct responses depending on the group, task and congruency revealed a main effect of congruency ($F(1,25) = 9.22$, $p = 0.006$, $\eta^2_p = 0.27$) (mean ± SD, Congruent 94.3 ± 1.9; Incongruent 92.2 ± 3.0) and a main effect of task ($F(1,25) = 6.31$, $p = 0.019$, $\eta^2_p = 0.20$) with higher accuracy in the shape-task compared to the texture-task in both groups (94.2 ± 2.7 and 92.3 ± 2.7, respectively) (see Fig. 2a/b). No significant interaction was observed.

According to differences between groups and tasks in the capacity of discrimination (assessed by *d'*), we again found a main effect of task ($F(1,25) = 4.95$, $p = 0.035$, $\eta^2_p = 0.17$) with a higher discrimination in the shape-task compared to the texture-task and a significant interaction of task and group ($F(1,25) = 4.86$, $p = 0.037$, $\eta^2_p = 0.16$). Since this interaction was significant, post hoc t-tests were conducted. We conducted paired-sample *t*-tests between tasks within each group and independent-sample t-tests between groups. Since four post hoc t-tests were performed, the significance threshold is set at $p = 0.0125$. Highly significant differences were found in the control group ($t(14) = 3.51$, $p = 0.003$, Cohen's d = 1.26) with a lower discrimination index for textures (d' = 2.4 ± 0.2) than for shapes (d' = 2.8 ± 0.4). In contrast, no differences between tasks were observed in the EB group ($t(11) = 0.01$, $p = 0.99$, Cohen's d = 0) (see Fig. 2c), thus showing equal performance. In addition, and as expected considering Fig. 2c, independent-sample t-tests between groups revealed a higher discriminability index in the texture task for EBs when compared to controls ($t(25) = 2.75$, $p = 0.011$, Cohen's d = 1.05, EBs *d'* = 2.8 ± 0.5; Controls *d'* = 2.4 ± 0.2). In contrast, no differences were found between groups for the shape discrimination task ($t(25) = 0.06$, $p = 0.95$, Cohen's d = 0).

3.2. ERP results

We inspected grand-average contact-locked ERPs in a selection electrodes from 50 ms pre-contact (baseline period) to 800 ms post-contact for (i) congruent trials, (ii) incongruent trials and (iii) a pool of both congruency conditions (congruent + incongruent trials). Across congruency conditions and tasks the mean number of included trials in the ERP analysis was 73.9 ± 6.2 (mean ± SD).

3.2.1. Texture discrimination

The mixed-model ANOVA revealed a main effect of congruency condition ($F(1,24) = 10.87$, $p = 0.003$, $\eta^2_p = 0.31$) indicating that the incongruence between the touched object and the heard word elicited a prominent negativity compared to the congruent condition (mean ± SD, Congruent: 5.9 ± 3.5 μV; Incongruent: 4.6 ± 3.3). Additionally, a significant 'electrode' x 'congruency' interaction ($F(3,62) = 3.22$, $\eta^2_p = 0.12$, $\varepsilon_{GG} = 0.59$, $p_{GG} = 0.035$) revealed differences in the topographical distribution of the incongruency effect (incongruent – congruent) for both groups. Furthermore, the 'electrode' x 'group' interaction (Greenhouse-Geisser corrected: $F(2,48) = 3.13$, $\eta^2_p = 0.12$, $\varepsilon_{GG} = 0.46$ $p_{GG} = 0.053$; Huyhn-Feldt corrected: $p_{HF} = 0.045$) suggested the existence of differences between groups on the scalp topography for both congruency conditions.

3.2.1.1. Congruent vs. incongruent conditions. Due to differences in the topographical distribution depending on the congruency condition and on the group when analyzing mean amplitude values in the 200–400 ms interval, below we analyse the onset latency of the incongruency effect (latency at which each group differed between congruent and incongruent trials) for each group separately.

3.2.1.1.1. EB group. For EBs, the difference between congruent and incongruent trials, as indexed by ten consecutive *t*-tests differing from zero, began at 168 ms in right frontal (F2, F4, F6, FC6) and right parietal-occipital sites (P2, P4, P6, PO2, PO4, PO6, O1, Oz, O2). The cluster-based permutation tests in the 100 ms time-window following the onset of the incongruence effect (168–268 ms) revealed a significant difference between congruent and incongruent conditions in a cluster very distributed all over the scalp ($p_{cluster\text{-}corrected} = 0.006$) (see the voltage map in the left panel of Fig. 3a). This difference was most pronounced over frontal,

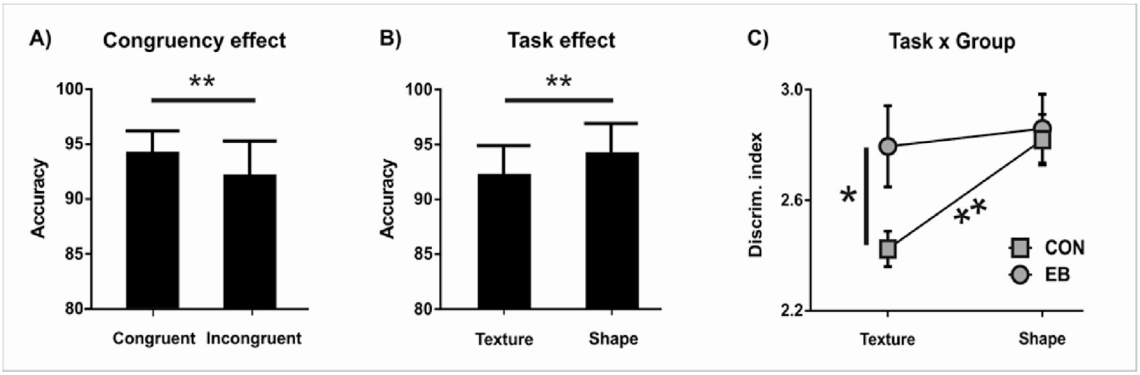

Fig. 2. A) Differences in the number of correct responses depending on trial congruency. B) Differences in the number of correct responses depending on the task. C) Differences in the discriminability index depending on the task and group. Notice the differences between groups in the texture discrimination task. CON: Sighted controls; EB: Early blind group. **p < 0.005, *p < 0.0125.

parietal-occipital and occipital electrodes (F2, F4, Fz, O2, PO6) [F2: $t(10) = 5.04$, Cohen's d = 0.53; F4: $t(10) = 4.41$, Cohen's d = 0.54; Fz: $t(10) = 4.21$, Cohen's d = 0.44; O2: $t(10) = 4.11$, Cohen's d = 0.60; PO6: $t(10) = 3.98$, Cohen's d = 0.62]. Despite observing such a distributed voltage, the scalp distribution of the CSD map revealed that the sources of activity were localized at right parietal-occipital electrodes (P4, P6, PO4, PO6, O1, Oz, O2) with the maximum effect in O2, PO6, Oz and PO4 [O2: $t(10) = 3.47$, $p_{uncorrected} = 0.006$, Cohen's d = 0.58; PO6: $t(10) = 3.22$, $p_{uncorrected} = 0.009$, Cohen's d = 0.45; Oz: $t(10) = 3.19$, $p_{uncorrected} = 0.009$, Cohen's d = 0.42; PO4: $t(10) = 3.01$, $p_{uncorrected} = 0.013$, Cohen's d = 0.42] (see the CSD map in the left panel of Fig. 3a). The white dots indicate the electrodes that were significantly different in that interval at $p_{uncorrected} < 0.05$.

3.2.1.1.2. Sighted controls. In sighted controls, congruent and incongruent trials started to differ at 228 ms at midline central-parietal locations (CP1, CPz, CP2, P1, Pz, P2). The cluster-based permutation tests in the 100 ms time-window following the onset of the incongruence effect (228–328 ms) revealed a significant difference between congruent and incongruent conditions in a cluster distributed over central-parietal electrodes ($p_{cluster\text{-}corrected} = 0.02$) [P5: $t(14) = 3.47$, Cohen's d = 0.37; P3: $t(14) = 3.22$, Cohen's d = 0.53; P1: $t(14) = 3.19$, Cohen's d = 0.57; Pz: $t(14) = 3.19$, Cohen's d = 0.60] (see the voltage map in the right panel of Fig. 3a). The scalp distribution of the CSD map localized the sources of the activity at slightly right-lateralized central and parietal locations (Cz, C2, CP1, CPz, CP2, CP4, Pz, P2) ($p_{cluster\text{-}corrected} = 0.02$) [CP2: $t(14) = 4.06$, Cohen's d = 0.10; CPz: $t(14) = 3.16$, Cohen's d = 0.29; CP4: $t(14) = 2.99$, Cohen's d = 0.22] (see the CSD map in the right panel of Fig. 3a).

3.2.1.2. EB group vs. sighted controls. The following section analyzes the onset latency of between group differences pooling together all trials (congruent + incongruent), since the electrophysiological activity corresponding to early stages of somatosensory processing is filtered out in the substraction of congruent from incongruent trials.

According to serial t-tests, differences between groups were found to arise at 76 ms frontocentral sites (FCz, FC2, Cz). Independent sample t-tests revealed that activity at frontal and frontocentral locations was significantly higher for EBs in the 100 ms-interval following the onset of the differences between groups (76–176 ms) [FC6: $t(24) = 2.43$, $p_{uncorrected} = 0.023$, Cohen's d = 0.99; FCz: $t(24) = 2.33$, $p_{uncorrected} = 0.028$, Cohen's d = 0.95; Fz: $t(24) = 2.23$, $p_{uncorrected} = 0.035$, Cohen's d = 0.91; FC2: $t(24) = 2.20$, $p_{uncorrected} = 0.037$, Cohen's d = 0.90] (see voltage map in Fig. 4a and b). The CSD maps during the 76–176 ms interval revealed that the previous frontocentral differences corresponded to the location of the sources of the activity (Fz, FCz, F1, F2, Cz, CPz, F6, F4 CP6) ($p_{cluster\text{-}corrected} = 0.004$) [Fz: $t(24) = 3.97$, Cohen's d = 1.59; FCz: $t(24) = 3.19$, Cohen's d = 1.24; F1: $t(24) = 3.09$, Cohen's d = 1.24; F2: $t(24) = 3.03$, Cohen's d = 1.20] (see CSD map of substraction in Fig. 4a). In addition, right occipital [O2: $t(24) = -3.09$, $p_{uncorrected} = 0.005$, Cohen's d = −1.30; PO6: $t(24) = -2.70$, $p_{uncorrected} = 0.012$, Cohen's d = −1.11; PO4: $t(24) = -2.09$, $p_{uncorrected} = 0.021$, Cohen's d = −0.85] and central-parietal [CP3, $t(24) = -2.48$, $p_{uncorrected} = 0.020$, Cohen's d = −1.02] sites were seen to corresponded to current sinks.

3.2.2. Shape discrimination

The mixed-model ANOVA in the shape discrimination task revealed a main effect of congruency condition ($F(1,24) = 13.92$, p = 0.001,

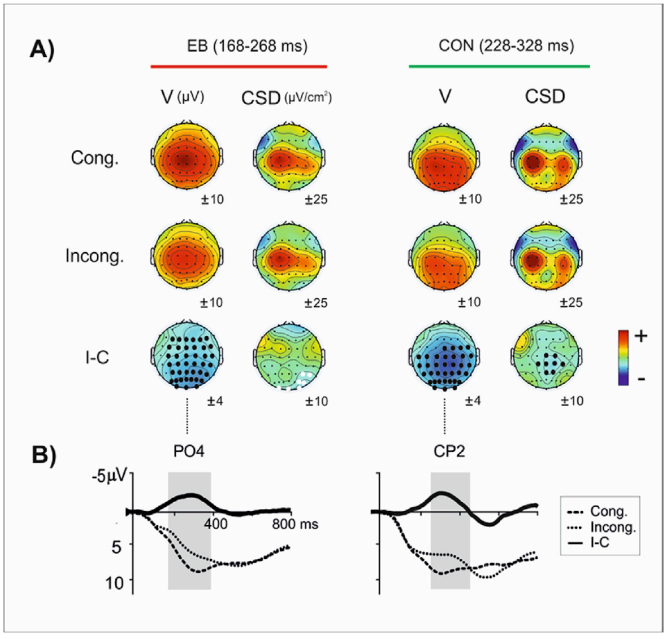

Fig. 3. A) Three–dimensional isovoltage topographical mappings (V) and the scalp distribution of the current source density (CSD), for the (i) congruent, (ii) incongruent and (iii) incongruent-congruent conditions in the texture discrimination task during a 100 ms time-window after the onset of discrimination. The number below each topographical map corresponds to the scale used (in μV units for voltage and μV/cm2 for CSD). The black dots indicate the electrodes that were significantly different ($p_{cluster\text{-}corrected} < 0.05$) between congruent and incongruent trials during the 100 ms time-window after the onset of discrimination. The white dots indicate the electrodes that were significantly different in that interval at $p_{uncorrected} < 0.05$. B) Grand-average contact-locked event-related potential (ERP) waveforms for congruent and incongruent conditions as well as the difference waveform (Incong.-Cong.; solid line) at PO4 and CP2 sites. The gray area indicates the time interval when the 2 congruency conditions differed statistically. CON: Sighted controls; CSD: Current source density; EB: Early blind group; I–C: incongruent-congruent; Sh: Shape; Tx: Texture; V: Voltage.

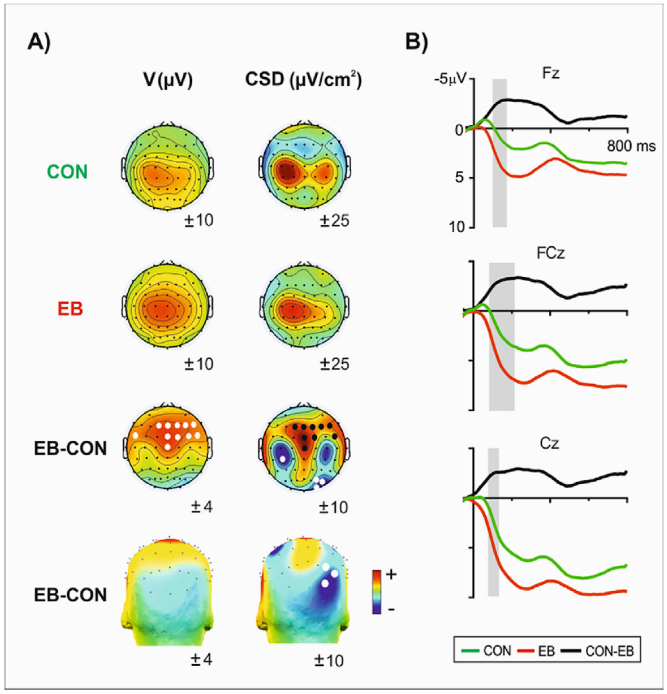

Fig. 4. A) Texture discrimination: Three-dimensional isovoltage topographical mappings (V) and the scalp distribution of the current source density (CSD), for the pool of both congruency conditions for the (i) sighted controls and (ii) early blind groups as well as (iii) their substraction–axial and coronal views– in a 100 ms time-window (76–176 ms) after the onset of the differences between groups. The black dots indicate the electrodes that were significantly different ($p_{cluster\text{-}corrected} < 0.05$) between groups during the time-interval reported above. The white dots indicate the electrodes that were significantly different in that interval at $p_{uncorrected} < 0.05$. B) Grand-average contact-locked event-related potential (ERP) waveforms for (i) controls (green line), (ii) EBs (red line) and (iii) their difference (black line) at Fz, C2A and O2 electrodes for the texture discrimination task. The gray area indicates the time interval where the 2 groups statistically differed.

$\eta^2_p = 0.37$) with incongruent trials showing overall more negative values than the congruent trials (mean ± SD, Congruent: 4.5 ± 3.6 μV; Incongruent: 3.0 ± 3.6). A significant 'electrode' x 'congruency' interaction ($F(3,73) = 5.11$, $\eta^2_p = 0.18$, $\varepsilon_{GG} = 0.69$, $p_{GG} = 0.003$) reflected differences in the topographical distribution of the incongruency effect. Although we did not find any significant interaction with the factor 'group', for comparison purposes only, an analogous analysis to the one conducted for the texture discrimination task (section 1 of the results) will be performed.

3.2.2.1. Congruent vs. incongruent conditions

3.2.2.1.1. EB group. In EBs, serial *t*-test revealed that differences between both congruency conditions started at 248 ms at right parietal sites (P6, PO6). A right central-parietal negativity extended up to occipital regions in the 100 ms time-window following the onset of the incongruence effect (248–348 ms) (see the voltage map in the left panel of Fig. 5a and b). However, the difference between congruent and incongruent conditions in this time-interval did not survive the correction for multiple comparisons. The maximum effect was found in (P06, P6, PO4 and O2) [PO6: $t(10) = 2.75$, $p_{uncorrected} = 0.020$, Cohen's d = 0.51; P6: $t(10) = 2.72$, $p_{uncorrected} = 0.021$, Cohen's d = 0.58; PO4: $t(10) = 2.54$, $p_{uncorrected} = 0.029$, Cohen's d = 0.43; O2: $t(10) = 2.53$, $p_{uncorrected} = 0.030$, Cohen's d = 0.40]. The sinks of the electrical activity were identified at right parietal sites [P6: $t(10) = 2.78$, $p_{uncorrected} = 0.019$, Cohen's d = 0.02; CP6: $t(10) = 2.60$, $p_{uncorrected} = 0.026$, Cohen's d = 0.31] (see CSD voltage map in the left panel of Fig. 5a).

3.2.2.1.2. Sighted controls. Sighted participants started to discriminate congruent and incongruent trials at 272 ms at right frontocentral (FC4, FC6), central (C2, C4, C6) and central-parietal sites (CP2, CP4, P6. Over the following 100 ms (272–372 ms) the topographical distribution showed a very widespread activity with nearly all scalp electrodes contributing to differ between both congruency conditions) ($p_{cluster\text{-}corrected} = 0.002$) (see the voltage map in the right panel of Fig. 5a and b). This incongruence effect was maximum at right central-parietal electrodes (CP6, P6, P4) [CP6: $t(14) = 5.28$, Cohen's d = 0.53; P6: $t(14) = 5.21$, Cohen's d = 0.56; P4: $t(14) = 5.16$, Cohen's d = 0.48]. The CSD maps during the 272–372 ms interval revealed that Cz, CPz, CP2, C2 and CP1 corresponded to the sinks of the electrical activity ($p_{cluster\text{-}corrected} = 0.026$) [Cz: $t(14) = 3.63$, Cohen's d = 0.20; CPz: $t(14) = 2.50$, Cohen's d = 0.23; CP2: $t(14) = 2.45$, Cohen's d = 0.23] (see CSD map in the right panel of Fig. 5a).

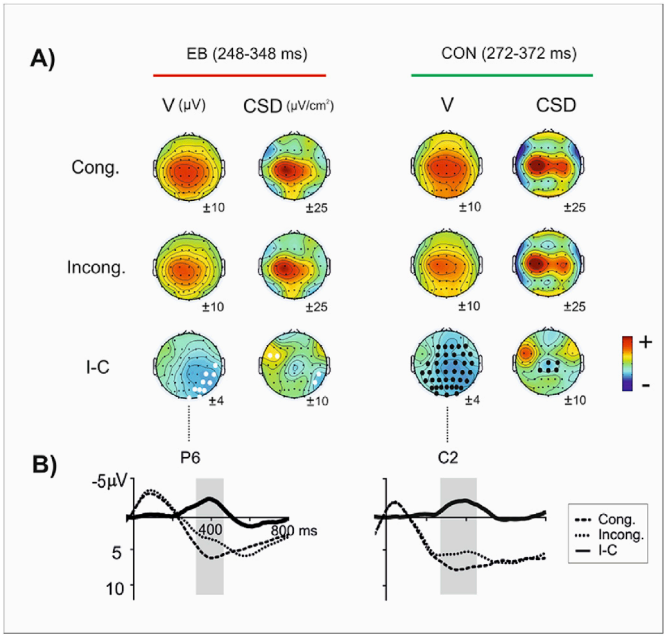

Fig. 5. A) Three–dimensional isovoltage topographical mappings (V) and the scalp distribution of the current source density (CSD), for the (i) congruent, (ii) incongruent and (iii) incongruent-congruent conditions in the shape discrimination task in a 100 ms time-window after the onset of discrimination. The number below each topographical map corresponds to the scale used (in μV units for voltage and μV/cm2 for CSD). The black dots indicate the electrodes that were significantly different ($p_{cluster\text{-}corrected} < 0.05$) between congruent and incongruent trials during the 100 ms time-window after the onset of discrimination. The white dots indicate the electrodes that were significantly different in that interval at $p_{uncorrected} < 0.05$. B) Grand-average contact-locked event-related potential (ERP) waveforms for congruent and incongruent conditions as well as the difference waveform (Incong.-Cong.; solid line) at P6 and C2 sites. The gray area indicates the time interval when the 2 congruency conditions differed statistically. CON: Sighted controls; CSD: Current source density; EB: Early blind group; I–C: incongruent-congruent; Sh: Shape; Tx: Texture; V: Voltage.

3.2.2.2. EB group vs. sighted controls. No differences between groups were found when pooling together all trials (congruent + incongruent).

4. Discussion

The present research analyzed neurophysiological differences on tactile processing between a group of EB individuals and sighted controls in two haptic discrimination tasks targeting microgeometric (texture) and macrogeometric (shape) properties. In line with previous research reporting superior tactile abilities in EBs during the processing of microgeometric attributes (Van Boven et al., 2000; Goldreich and Kanics, 2003), our behavioral data showed that EBs presented superior discriminability abilities in a texture discrimination task compared to sighted controls. Importantly, no differences between groups were found in the capacity to discriminate shapes. The specific neural signatures underlying the enhanced skills found in the EB group during texture discrimination were assessed by electrophysiological measures, revealing that EBs started to present more positive cortical activity at frontocentral locations (and more negative values at occipital sites) around 75 ms. Moreover, the comparison of congruent and incongruent trials allowed us to determine the onset of the discrimination process in EBs for both micro- (EB: 170 ms) and macrogeometric (EB: 250 ms) properties (see for similar approaches, Thorpe et al., 1996; Rodríguez-Fornells et al., 2002).

The temporal information and the spatial distribution of the cortical activity corresponding to differences between groups are important in order to understand the mechanisms leading EBs to have enhanced skills during the processing of microgeometric properties. Taking into account that somatosensory information can be delivered to the cortex within a range of 15–30 ms (Mauguiere et al., 1999; Palva et al., 2005) and that the time required to discriminate expected and unexpected textures is at least 170 ms (according to the results reported here), the latency at which the first group differences appear (~75 ms) might correspond to initial stages of somatosensory processing carried out in primary sensory regions. In accordance with this notion, scalp recorded somatosensory ERP components within the first 100 ms were found to be generated in the primary somatosensory area (S1) (Allison et al., 1992). Only after 120 ms, the neural generators of somatosensory evoked potentials were located in higher order sensory regions (e.g., secondary somatosensory areas). Thus, according to this temporal pattern, one of the underlying reasons contributing to a more efficient processing in EBs during texture discrimination might be related to cortical reorganization occurring in regions associated with the intact modalities (e.g., somatosensory), such as an enlarged representation of the reading finger in the S1 of Braille readers (Pascual-Leone and Torres, 1993; Sterr et al., 1998). The spatial distribution of the differences between groups converges with this idea, since the source density maps revealed bilateral differences between groups in presumably somatosensory areas, at central locations (see Fig. 4). Still, it seems unlikely that the group differences found during texture discrimination were solely driven by enlarged representations in S1, since this would also lead to differences during shape discrimination considering that all types of somatosensory input are first conveyed to S1.

Plastic reorganization in EBs could also occur in areas initially responsible for the deprived sense since occipital areas (normally recruited for visual processing in sighted population) have been shown to subserve tactile processing (Burton et al., 2006; Pietrini et al., 2004; Sadato et al., 1996). Importantly, the involvement of occipital regions in EBs has been related to the processing of both micro- (Braille reading) and macrogeometric properties (width and angle discrimination) (Sadato et al., 1998). Our results support this idea bearing in mind that the incongruence effect elicited a prominent negativity at occipital regions in the EB group in both discrimination tasks (see Figs. 3 and 5). Likewise, we found differences between groups at right occipital sites with EBs presenting more negative values than sighted controls pooling together all conditions (see Fig. 4). Similar posterior negative deflections present in EBs have been previously reported during tactile oddball tasks (Roder et al., 1996), tactile reading tasks (Uhl et al., 1991) and tactile mental imagery (Uhl et al., 1994), associating these patterns of occipital responses with both high-level cognitive processing and low-level sensory discrimination. Lastly, cortico-cortical connections could as well mediate crossmodal plasticity in blind individuals considering that increased connectivity between S1 and occipital cortices has been previously reported in EBs (Wittenberg et al., 2004).

While the above-mentioned speaks on the relevance of occipital areas in EBs during somatosensory processing (for both micro- and macrogeometric properties), occipital areas seem to be equally relevant in sighted population for the processing of macrogeometric attributes as a result of visual mechanisms. Importantly, in sighted population the preferred sensory modality to encode shape-relevant information is vision, whereas texture is mainly encoded using touch (Lederman and Klatzky, 1987; Lederman et al., 1996). These two factors may account for the absence of differences between groups in the shape discrimination task. Thus, in EBs somatosensory and visual (due to cortical reorganization) areas seem to be highly active during texture and shape processing. However, during shape discrimination in sighted individuals similar occipital activations might be related to visual mechanisms. Notably, the topographical maps for the incongruence effect in the shape discrimination task highly resemble between groups (see Fig. 5) and this resemblance is not shared in the texture-task (Fig. 3). Visual imagery and shared visuo-tactile shape representations are some of the visual strategies from which sighted participants could benefit.

Evidence supporting the role of visual imagery in haptic shape perception comes from studies in which individual differences in the degree of haptic shape-selective activity in the right LOC have been seen to correlate with ratings of imagery-vividness (Zhang et al., 2004) and activations evoked by visual imagery were found to be more correlated with those evoked by the haptic perception of familiar (compared to unfamiliar) shapes (Lacey et al., 2010). Effective connectivity analyses converged with these findings showing that visual imagery and haptic perception of familiar shapes activated similar networks whereas unfamiliar shape perception did not (Deshpande et al., 2010) (for a review see Lacey and Sathian, 2014). Furthermore, the lateral occipital tactile-visual area (LOtv) is thought to store bimodal shape representations that can be accessed either by vision or haptics (Amedi et al., 2001; Amedi et al., 2002). In this line, visual representations available in sighted individuals could be used to enrich bimodal object-representation stored in this region, and because this improved representation is shared across both modalities, the haptic system might benefit from it during the haptic discrimination process. As these shared representations are specific for objects but not for textures, our results match well with the idea that compensatory mechanisms are present only during shape processing. However, the present study lacks direct evidence concerning the role of visual representations during shape discrimination and further studies would be needed to address this issue. Similar to other studies (Lacey and Campbell, 2006; Lawson et al., 2015), the access to visual representations during haptic discrimination could be blocked conducting a concurrent or dual task since spatial coding has been found to be of great importance to maintain accurate haptic shape representations (Lawson et al., 2015).

Summing up, this is the first study to show early differences between EB and sighted individuals in the electrophysiological signatures of texture (but not shape) discrimination and we hypothesize that the lack of differences between groups in the shape discrimination task might be explained by similar occipital activations in EBs (due to cortical reorganization related to visual deprivation) and in sighted controls (due to visual mechanisms).

Competing interests

The authors declare no disclosure of financial interests or potential conflict of interest.

Acknowledgements

The authors thank all the people that participated in the study, the Catalan Organization for the integration blind people (ACIC), the National Organization of Spanish blind people (ONCE) and David Cucurell for his help during the recordings. This work was supported by a Spanish government grant to ARF (PSI2015-69178-P) and a predoctoral grant (MINECO-FPI program) from the Spanish government awarded to AGA.

References

Alary, F., Duquette, M., Goldstein, R., Elaine, C.C., Voss, P., La Buissonniere-Ariza, V., et al., 2009. Tactile acuity in the blind: a closer look reveals superiority over the sighted in some but not all cutaneous tasks. Neuropsychologia 47, 2037–2043.
Alary, F., Goldstein, R., Duquette, M., Chapman, C.E., Voss, P., Lepore, F., 2008. Tactile acuity in the blind: a psychophysical study using a two-dimensional angle discrimination task. Exp. Brain Res. 187, 587–594.
Allison, T., McCarthy, G., Wood, C.C., 1992. The relationship between human long-latency somatosensory evoked potentials recorded from the cortical surface and from the scalp. Electroencephalogr. Clin. Neurophysiol. 84, 301–314.
Amedi, A., Jacobson, G., Hendler, T., Malach, R., Zohary, E., 2002. Convergence of visual and tactile shape processing in the human lateral occipital complex. Cereb. Cortex 12, 1202–1212.
Amedi, A., Malach, R., Hendler, T., Peled, S., Zohary, E., 2001. Visuo-haptic object-related activation in the ventral visual pathway. Nat. Neurosci. 4, 324–330.
Bohlhalter, S., Fretz, C., Weder, B., 2002. Hierarchical versus parallel processing in tactile object recognition: a behavioural-neuroanatomical study of aperceptive tactile agnosia. Brain 125, 2537–2548.
Burton, H., McLaren, D.G., Sinclair, R.J., 2006. Reading embossed capital letters: an fMRI study in blind and sighted individuals. Hum. Brain Mapp. 27, 325–339.
Cappagli, G., Cocchi, E., Gori, M., 2017. Auditory and proprioceptive spatial impairments in blind children and adults. Dev. Sci. 20.
Cunillera, T., Gomila, A., Rodriguez-Fornells, A., 2008. Beneficial effects of word final stress in segmenting a new language: evidence from ERPs. BMC.Neurosci. 9, 23.
Delorme, A., Makeig, S., 2004. EEGLAB: an open source toolbox for analysis of single-trial EEG dynamics including independent component analysis. J. Neurosci. Methods 134, 9–21.
Delorme, A., Sejnowski, T., Makeig, S., 2007. Enhanced detection of artifacts in EEG data using higher-order statistics and independent component analysis. Neuroimage 34, 1443–1449.
Deshpande, G., Hu, X., Lacey, S., Stilla, R., Sathian, K., 2010. Object familiarity modulates effective connectivity during haptic shape perception. Neuroimage 49, 1991–2000.
Forster, B., Eardley, A.F., Eimer, M., 2007. Altered tactile spatial attention in the early blind. Brain Res. 1131, 149–154.
Girden, E.R., 1992. ANOVA: Repeated Measures (Quantitative Applications in the Social Sciences). By MLews-beck. SAGE Publications, Newbury Park, California.
Goldreich, D., Kanics, I.M., 2003. Tactile acuity is enhanced in blindness. J. Neurosci. 23, 3439–3445.
Gori, M., Sandini, G., Martinoli, C., Burr, D., 2010. Poor haptic orientation discrimination in nonsighted children may reflect disruption of cross-sensory calibration. Curr. Biol. 20, 223–225.
Gori, M., Sandini, G., Martinoli, C., Burr, D.C., 2013. Impairment of auditory spatial localization in congenitally blind human subjects. Brain 137, 288–293.
Grant, A.C., Thiagarajah, M.C., Sathian, K., 2000. Tactile perception in blind Braille readers: a psychophysical study of acuity and hyperacuity using gratings and dot patterns. Percept. Psychophys. 62, 301–312.
Gurtubay-Antolin, A., Rodriguez-Herreros, B., Rodriguez-Fornells, A., 2015. The speed of object recognition from a haptic glance: event-related potential evidence. J. Neurophysiol. 113, 3069–3075.
Heller, M.A., 1989. Texture perception in sighted and blind observers. Percept. Psychophys. 45, 49–54.
Huynh, H., Feldt, L.S., 1976. Estimation of the Box correction for degrees of freedom from sample data in randomized block and split-plot designs. J. Educ. Stat. 1, 69–82.
Jasper, H.H., 1958. The ten twenty electrode system of the international federation. Electroencephalogr. Clin. Neurophysiol. 10, 371–375.

Jennings, R.J., Wood, C.C., 1976. The +øΓÇÉAdjustment procedure for RepeatedΓÇÉMeasures analyses of variance. Psychophysiology 13, 277–278.
Johnson, M., 1997. Proceeding of the Medical Image Computing and Computer-assisted Interventation (MICCAI98). Blackwell, Cambridge, MA.
Kayser, J., Tenke, C.E., 2006. Principal components analysis of laplacian waveforms as a genetic method for identifying ERP generator patterns: I. Evaluation with auditory oddball tasks. Clin. Neurophysiol. 117, 348–368.
Klatzky, R.L., Lederman, S.J., 1995. Identifying objects from a haptic glance. Percept. Psychophys. 57, 1111–1123.
Lacey, S., Campbell, C., 2006. Mental representation in visual/haptic crossmodal memory: evidence from interference effects. Q. J. Exp. Psychol. 59, 361–376.
Lacey, S., Flueckiger, P., Stilla, R., Lava, M., Sathian, K., 2010. Object familiarity modulates the relationship between visual object imagery and haptic shape perception. Neuroimage 49, 1977–1990.
Lacey, S., Sathian, K., 2014. Visuo-haptic multisensory object recognition, categorization, and representation. Front. Psychol. 5, 730.
Lawson, R., Fernandes, A.M., Albuquerque, P.B., Lacey, S., 2015. Remembering Touch: Using Interference Tasks to Study Tactile and Haptic Memory. In: Mechanisms of Sensory Working Memory: Attention and Perfomance XXV, vol. 239.
Lederman, S.J., Klatzky, R.L., 1987. Hand movements: a window into haptic object recognition. Cogn. Psychol. 19, 342–368.
Lederman, S.J., Klatzky, R.L., 1990. Haptic classification of common objects: knowledge-driven exploration. Cogn. Psychol. 22, 421–459.
Lederman, S.J., Klatzky, R.L., 1993. Extracting object properties through haptic exploration. Acta Psychol. (Amst) 84, 29–40.
Lederman, S.J., Summers, C., Klatzky, R.L., 1996. Cognitive salience of haptic object properties: role of modality-encoding bias. Perception 25, 983–998.
Lewald, J., 2002. Vertical sound localization in blind humans. Neuropsychologia 40, 1868–1872.
Maris, E., Oostenveld, R., 2007. Nonparametric statistical testing of EEG- and MEG-data. J. Neurosci. Methods 164, 177–190.
Mauguiere, F., Allison, T., Babiloni, C., Buchner, H., Eisen, A.A., Goodin, D.S., et al., 1999. Somatosensory evoked potentials. The Int. Fed. Clin. Neurophysiol. 52 (Electroencephalogr. Clin. Neurophysiol. Suppl), 79–90.
Merabet, L.B., Pascual-Leone, A., 2010. Neural reorganization following sensory loss: the opportunity of change. Nat. Rev. Neurosci. 11, 44–52.
Noppeney, U., Friston, K.J., Ashburner, J., Frackowiak, R., Price, C.J., 2005. Early visual deprivation induces structural plasticity in gray and white matter. Curr. Biol. 15, R488–R490.
Oostenveld, R., Fries, P., Maris, E., Schoffelen, J.M., 2011. FieldTrip: open source software for advanced analysis of MEG, EEG, and invasive electrophysiological data. Comput. Intell. Neurosci. 2011, 156869.
Palva, S., Linkenkaer-Hansen, K., Naatanen, R., Palva, J.M., 2005. Early neural correlates of conscious somatosensory perception. J. Neurosci. 25, 5248–5258.
Pan, W.J., Wu, G., Li, C.X., Lin, F., Sun, J., Lei, H., 2007. Progressive atrophy in the optic pathway and visual cortex of early blind Chinese adults: a voxel-based morphometry magnetic resonance imaging study. Neuroimage 37, 212–220.
Pascual-Leone, A., Torres, F., 1993. Plasticity of the sensorimotor cortex representation of the reading finger in Braille readers. Brain 116 (Pt 1), 39–52.
Peña-Casanova, J., 1999. Intervención cognitiva en la enfermedad del Alzheimer. Fundación La Caixa, Barcelona.
Perrin, F., Pernier, J., Bertrand, O., Echallier, J.F., 1989. Spherical splines for scalp potential and current density mapping. Electroencephalogr. Clin. Neurophysiol. 72, 184–187.
Pietrini, P., Furey, M.L., Ricciardi, E., Gobbini, M.I., Wu, W.H., Cohen, L., et al., 2004. Beyond sensory images: object-based representation in the human ventral pathway. Proc. Natl. Acad. Sci.U.S.A 101, 5658–5663.
Roder, B., Rosler, F., Hennighausen, E., Nacker, F., 1996. Event-related potentials during auditory and somatosensory discrimination in sighted and blind human subjects. Brain Res. Cogn. Brain Res. 4, 77–93.
Rodríguez-Fornells, A., Kurzbuch, A.R., Münte, T.F., 2002. Time course of error detection and correction in humans: neurophysiological evidence. J. Neurosci. 22 (22), 9990–9996.
Sadato, N., Pascual-Leone, A., Grafman, J., Deiber, M.P., Ibanez, V., Hallett, M., 1998. Neural networks for Braille reading by the blind. Brain 121 (Pt 7), 1213–1229.
Sadato, N., Pascual-Leone, A., Grafman, J., Ibanez, V., Deiber, M.P., Dold, G., et al., 1996. Activation of the primary visual cortex by Braille reading in blind subjects. Nature 380, 526–528.
Sterr, A., Green, L., Elbert, T., 2003. Blind Braille readers mislocate tactile stimuli. Biol. Psychol. 63, 117–127.
Sterr, A., Muller, M.M., Elbert, T., Rockstroh, B., Pantev, C., Taub, E., 1998. Perceptual correlates of changes in cortical representation of fingers in blind multifinger Braille readers. J. Neurosci. 18, 4417–4423.
Thorpe, S, Fize, D, Marlot, C., 1996. Speed of processing in the human visual system. Nature 381 (6582), 520–522.
Uhl, F., Franzen, P., Lindinger, G., Lang, W., Deecke, L., 1991. On the functionality of the visually deprived occipital cortex in early blind persons. Neurosci. Lett. 124 (2), 256–259.
Uhl, F., Kretschmer, T., Lindinger, G., Goldenberg, G., Lang, W., Oder, W., Deecke, L., 1994. Tactile mental imagery in sighted persons and in patients suffering from peripheral blindness early in life. Electroencephalography Clin. Neurophysiol. 91 (4), 249–255.
Van Boven, R.W., Hamilton, R.H., Kauffman, T., Keenan, J.P., Pascual-Leone, A., 2000. Tactile spatial resolution in blind braille readers. Neurology 54, 2230–2236.
Vercillo, T., Burr, D., Gori, M., 2016. Early visual deprivation severely compromises the auditory sense of space in congenitally blind children. Dev. Psychol. 52, 847–853.
Voss, P., Collignon, O., Lassonde, M., Lepore, F., 2010. Adaptation to sensory loss. Wiley. Interdiscip. Rev. Cogn. Sci. 1, 308–328.
Wan, C.Y., Wood, A.G., Reutens, D.C., 2010. Congenital blindness leads to enhanced vibrotactile perception. Neuropsychologia 48, 631–635.
Wittenberg, G.F., Werhahn, K.J., Wassermann, E.M., Herscovitch, P., Cohen, L.G., 2004. Functional connectivity between somatosensory and visual cortex in early blind humans. Eur. J. Neurosci. 20, 1923–1927.
Zhang, M., Weisser, V.D., Stilla, R., Prather, S.C., Sathian, K., 2004. Multisensory cortical processing of object shape and its relation to mental imagery. Cogn. Affect. Behav. Neurosci 4, 251–259.